COMPARISON BETWEEN MODELS OF TWO AND THREE PHASES IN THE SIMULATION OF DRYING IN FLUIDIZED BED

J.F.A. Vitor, joaofrancisco@dppg.cefetmg.br
J.F.L. Souza, jleonciofs@gmail.com
CEFET-MG/DPPG– CEP 30.280-000 – Av. Amazonas 5253 – Nova Suissa, Belo Horizonte – MG – Brazil – Fax +55 (31)3319-7023, 3319-6805

Abstract. *The modeling of the drying operation allows the simulation of the process as well as the estimation of heat and mass transfer coefficients related to the gas and solid phases. The objective of this study is to compare the performance of two models describing the diffusive drying of tapioca in a fluidized bed. The first model considers the bed as constituted by two phases – solid and gas – both in perfect mixture. The second model considers the presence of three phases: a solid phase, assumed as well mixed; a bubble phase with exclusively convective transfer mechanism; and an interstitial gas phase with convective and diffusive transport phenomena.*
The two models presented similar performances. However, the predictive capacity of the three phases model is superior due the fact that this model is based on fundamental characteristics of the components involved in the process.

Keywords: *fluidized bed dryer; batch drying; algebraic-differential approach.*

1. INTRODUCTION

Several models are found in the literature to describe the drying of porous particulate materials in fluidized bed. Normally these models are classified through the number of phases considered as present in the bed.

The modeling of the drying of porous bodies in two phases – solid and gas – is based on the theory of the Truesdell (1957) mixture. The equations of this model are presented in Biscaia Jr. et al. (1996), describing the momentum, mass and energy balances in both phases.

The model of the two phases has been used to describe the drying in different configurations: fixed bed, moving bed, crossed flow dryers, etc. Calado (1993) used this approach to describe the drying of corn and soy in fixed and moving bed with concurrent flows and crossed flows and Calçada (1994)used the two phases model in the drying of corn conducted fixed bed equipment. Mancini (1996) considered different models, amongst them the two phase model for the description of the transference of mass in the drying of grains. Valença and Massarani (2000) simulated the drying of corn in cross- and counter-current flow dryers using the two phases model resulting in good agreement with experimental data.

The two phases model has also been adopted in the modeling of drying in fluidized bed. Kerkhof (1994), Wang and Chen (2000), Lima (2004) considered both the solid phase and the gaseous phase as well mixed.

A second group of authors considered the presence of bubbles inside the fluidized bed, resulting in the three phases models: the solid phase, the interstitial gas phase and the bubble gas phase. Hoebink and Rietema (1980-a) considered the temperature and the moisture in each phase as homogenous. Diffusive models have been used by Hoebink and Rietema (1980-b), Zahed et al. (1995) to describe the moisture profiles in the interior of the particles. Wildhagen et al. (2002) modeled the drying of porous particles of capilar structure – alumina – considering the solid phase as well mixed and interstitial and bubble gas phases as a pure plug-flow. Vitor (2003) and Rizzi (2007), modeling the drying of a bioproduct with celular structure in a fluidized bed dryer, considered thre phases: the solid phase assumed as well mixed; the bubble phase assumed as purely convective (plug flown assumption) and the interstitial gas phase with convective and difusive transport mechanisms.

The purpose of this work is to compare the performance of two models used to describe the drying of *tapioca* in fluidized bed. The first model only considers the energy and mass global balances, as presented by Lima (2004). The second model is a three phases model where empirical forms of the heat and mass transfer coefficients are used to describe the transfer mechanisms between the interstitial and bubble gas.

2. THREE-PHASE MODEL

The three-phase fluidized bed dryer model – solid, interstitial gas and bubble gas (Fig. 1) – considers gas composed of air and water vapor, and the solid by the particulate material and the liquid water. The model equations express the mass and energy balances in each phase.

This three-phase model (Vitor, 2003) is based on the assumption that solids are perfectly mixed, while bubbles are moving upwards in plug flow through the column. The interstitial gas phase is regarded as a dispersion model. According to such formulation, the heat loss from the bed to the environment occurs only with the interstitial gas phase.

The main assumptions of the model are: (a) all transport mechanisms presented in the bubble gas phase are purely convective and unidirectional; (b) the energy and mass transfer between solid and bubble gas phases are neglected; (c) the interstitial gas porosity is equal to the minimum fluidization porosity.

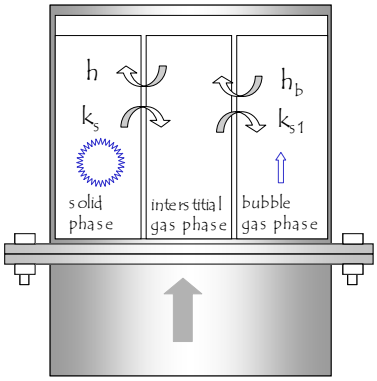

Figure 1. Transfer coefficient between phases.

The equations of the mass and energy balances in the solid particulate, interstitial gas and bubble gas phases are:

2.1. Solid phase

$$(1-\varepsilon)\rho_s \frac{d}{dt} Y_s = -f_{M1} \tag{1a}$$

$$(1-\varepsilon)\rho_s \frac{d}{dt} H_{su} = f_{E1} - f_{M1}\left(H_u + \lambda_u\right) \tag{1b}$$

$$H_{su} = H_s + H_u Y_s \tag{1c}$$

where ε is the bed porosity, ρ, density, Y, moisture content in dry basis, f_{M1}, local mass transfer rate between solid phase and interstitial gas, f_{E1}, local heat transfer rate between solid phase and interstitial gas, H is the specific enthalpy, λ, latent heat of vaporization, *s,* solid and *u* is the liquid water.

2.2. Interstitial gas phase

$$\frac{d}{dt}\overline{Y}_{gi} + G_{gi}\beta_y \frac{\overline{Y}_{gi} - Y_{gi0}}{L} = f_{M1} - f_{M2T} \tag{1d}$$

$$(1-\delta)\varepsilon_{mf}\rho_g \frac{d}{dt}\overline{H}_i + G_{gi}\beta_T \frac{\overline{H}_i - H_0}{L} = f_{E2T} - f_{E1} + f_{M1}\left(H_u + \lambda_u\right) - f_{M2T} H_{vi} - E_w \tag{1e}$$

$$\overline{H}_i = \overline{H}_{gi} + \overline{H}_{vi}\overline{Y}_{gi} \tag{1f}$$

where G is the superficial mass flow rate, β is the coefficient related to the dispersion in the interstitial gas phase, f_{M2T}, the global mass transfer rate between solid phase and interstitial gas, δ, the bubble porosity, L is the height of the bed, f_{M2}, the heat transfer rate between interstitial and bubble gas, E_w, the rate of heat dissipated through wall, *gi*, interstitial gas, *vi*, vapor water, *0*, initial conditions and *mf* is the minimum fluidization.

2.3 – bubble gas phase

$$\delta\rho_g \frac{\partial}{\partial t} Y_{gb} + G_{gb} \frac{\partial}{\partial z} Y_{gb} = f_{M2} \tag{1g}$$

$$\delta\rho_g \frac{\partial}{\partial t} H_b + G_{gb} \frac{\partial}{\partial z} H_b = f_{M2} H_{vi} - f_{E2} \tag{1h}$$

$$H_b = H_{gb} + H_{vb} Y_{gb} \tag{1i}$$

where *gb* is the bubble gas, f_{M2} is the local mass transfer rate between interstitial and bubble gas, f_{E2} is the local heat transfer rate between interstitial and bubble gas,

The enthalpies are related with the temperature through the expressions:

$$H_S = C_{pS}\left(T_S - T_R\right) \qquad H_U = C_{pU}\left(T_S - T_R\right)$$

$$H_{Gi} = C_{pG}(T_{Gi} - T_R) \qquad H_{Vi} = \lambda_o + C_{pv}(T_{Gi} - T_R)$$

$$H_{Gb} = C_{pG}(T_{Gb} - T_R) \qquad H_{Vb} = \lambda_o + C_{pv}(T_{Gb} - T_R)$$

where C_p is the specific heat at constant pressure and T is the temperature. The following initial and boundary conditions are presented:

$$Y_s(0) = Y_{s0} \tag{2a}$$

$$T_s(0) = T_{s0} \tag{2b}$$

$$Y_{Gi}\left(0,z\right) = Y_{Gb}\left(0,z\right) = Y_{G0} \tag{2c}$$

$$T_{Gi}\left(0,z\right) = T_{Gb}\left(0,z\right) = T_{G0} \tag{2d}$$

$$Y_{Gi}\left(t,0\right) = Y_{Gb}\left(t,0\right) = Y_{G0} \tag{2e}$$

$$T_{Gi}\left(t,0\right) = T_{Gb}\left(t,0\right) = T_{G0} \tag{2f}$$

In the interstitial gas equations the enthalpy and concentration axial profiles are approximated by simple parabolic profiles. Based on this approximation, the mass and energy balances of this phase are adjusted by two dimensionless parameters, β_Y and β_T, that vary in the domain [1,3/2]. In the lower limit, $\beta \to 1$, the parabolic profiles degenerate, tending to a constant profile (analogous to the perfect stirred model).

In Tab. 1 the expressions of the heat and mass transfer rates presented in the mass and heat balances, the *f* functions in Eqs. (1-a) to (1-i), are presented, where *ha* is the effective volumetric heat transfer coefficient between solid phase and interstitial gas, $k_S a$ is the effective volumetric mass transfer coefficient between solid phase and interstitial gas, Y_s^* is the equilibrium moisture content of the tapioca in dry basis, $h_b a_1$ is the effective volumetric heat transfer coefficient between interstitial and bubble gas, $k_{S1} a_1$ is the effective volumetric mass transfer coefficient between interstitial and bubble gas, and *N*, the number of axial discretization intervals.

Table 1. The heat and mass transfer rates per unit of porous medium volume.

$f_{E1} = ha\left(T_{gi} - T_s\right)$	$f_{M1} = k_s a\left(Y_s - Y_s^*\right)$
$f_{E1T} = \frac{1}{N}\sum_{k=1}^{N} f_{E1}^{(k)}$	$f_{M1T} = \frac{1}{N}\sum_{k=1}^{N} f_{M1}^{(k)}$
$f_{E2} = h_b a_1\left(T_{gb} - T_{gi}\right)$	$f_{M2} = k_{s1} a_1\left(Y_{gi} - Y_{gb}\right)$
$f_{E2T} = \frac{1}{N}\sum_{k=1}^{N} f_{E2}^{(k)}$	$f_{M2T} = \frac{1}{N}\sum_{k=1}^{N} f_{M2}^{(k)}$

3. FLUIDIZED BED PROPERTIES

The drag force on the particles, in the case of isotropic, homogeneous porous media percolated by the incompressible flow of an ideal gas, is modeled by Darcy's equation (Eq. 3)

$$-\frac{dp}{dz} = \frac{\mu q}{k} + \frac{c\rho q^2}{\sqrt{k}} \tag{3}$$

which, in the case of an isothermal perfect gas, when integrated, is reduced to Eq (4)

$$\frac{\overline{\rho}}{G}\left(-\frac{\Delta p}{L}\right) = \frac{\mu}{k} + \frac{c}{\sqrt{k}}G \tag{4}$$

where $G = \rho q$, $\overline{\rho} = \frac{\rho_1 + \rho_2}{2} = \frac{M}{RT}\left(p_2 - \frac{\Delta p}{2}\right)$ e $\Delta p = p_2 - p_1$, k is the bed permeability [m^2], c is the form factor [adim], μ is the viscosity of the air [kg/ms], G_g is the mass flow of the gas [kg/m^{2}s], Δp is the drop in pressure [N/m^2], ρ_1 and ρ_2 are the densities of the air in and out of the bed, respectively [kg/m^3] and L is the height of the bed. The form factor, c, and the permeability, k, are therefore calculated by using the permeametry (Massarani, 1997). This correlates a set of experimental measures of the pressure drop related to the flow of the air, carried out on a permeameter.

The Blake-Kózeny or Kózeny-Càrmàn equation correlates, in the capillary model, the permeability with the properties of the particles and the porosity of the bed, where the sphericity of the particles (ϕ) is achieved.

$$k = \frac{\left(d_p\phi\right)^2 \varepsilon^3}{36\beta\left(1-\varepsilon\right)^2} \text{ , where } \beta \equiv 4.5. \tag{5}$$

The specific surface of solid particles in contact with the interstitial gas can be calculated through the expression

$$a = \frac{6\left(1-\varepsilon_{mf}\right)}{d_p\phi} \tag{6}$$

The bubbles porosity and the specific area of the bed are determined according to Eqs. (7) and (8), where d_p is the particle diameter and ϕ is the sphericity.

$$\delta = \frac{\varepsilon - \varepsilon_{mf}}{1-\varepsilon_{mf}} \tag{7}$$

$$a = \frac{6\left(1-\varepsilon_{mf}\right)}{d_p\,\phi} \tag{8}$$

The specific mass flow of each phase is calculated by Eqs. (9) and (10)

$$G_{Gb} = \psi\left(G_G - G_{mf}\right) \tag{9}$$

$$G_{Gi} = G_G - G_{Gb} \tag{10}$$

where, due to the fact that the particles of tapioca having been characterized between the Geldart ranges A and B, the flow of gas of each phase is corrected by the coefficient Ψ=0,67 (Hilligardt and Werther, 1986).

The water specific heat in the used temperature ranges can be considered constant and equal to 4186 J kg^{-1} K^{-1}.

The air thermal conductivity (k_g) and the vapor diffusivity in the air (D_{ab}) as functions of the temperature were determined by Pakowski et al. (1991) and are presented in Eqs. (11) and (12).

$$k_g = 2,42503 \cdot 10^{-2} + 7,88913 \cdot 10^{-5} T_g - 1,79034 \cdot 10^{-8} {T_g}^2 - 8,57050 \cdot 10^{-12} {T_g}^3 \tag{11}$$

$$D_{ab} = 21,6 \cdot 10^{-2} \left(\frac{T_g}{20} \right)^{1,8} . \tag{12}$$

Heat is dissipated through the wall owing to the difference between the gas temperature inside the bed and ambient temperature of the air. The correspondent rate, E_w, is expressed by

$$E_w = \frac{\alpha_w}{V_{bed}} (\overline{T}_{bed} - T_\infty) \tag{13}$$

where α_w is the heat transfer coefficient through bed wall, V_{bed} is the volume of the fluidized bed. Mass and heat transfer coefficients between interstitial and bubble gas phases, h_b and k_{S1}, respectively, may be estimated from the equations presented in Kunii and Levenspiel (1991) and Palàncz (1982).

According to Hilligardt and Werther (1978), in fluidized beds with perforated plaque distributor using Geldart solids type A or B, the diameter of the bubbles can be calculated through

$$d_b = 1,43 \left[A_L \left(\frac{G_G - G_{Gmf}}{\rho_g} \right) \right]^{0,4} g^{-0,2} + 2,7x10^{-2} z \left(\frac{G_G - G_{Gmf}}{\rho_g} \right)^{0,94} \tag{14}$$

After the discretization of the axial derivatives presented in the above equations, the resulting model equations are a system of algebraic-differential equations that was numerically solved by the computational code DASSL (Petzold, 1989).

4. TWO PHASES MODEL

The two phases drying model considers only the solid phase – dry solid and liquid water – and one gas phase – air and water vapor. This model has been widely used to describe the drying process conducted in fixed and moving beds (Calado, 1993, Calçada, 1998, Mancini, 1996, amongst others), the same model was used by Lima (2004) in the modeling of the fluidized bed drying of polyhydroxybutirate (PHB). This model can be interpreted as resulted by the spatial variable integration of the three phases model and, in spite of being able to present satisfactory adjustment capacity to real experimental data, its predictive capacity is very limited.

This two phases model considers both the phases as well mixed. Apart from this simplification, the model considers the same temperature for both phases inside the bed. The equations of the model are

4.1 – mass balance

$$\frac{W_{ds}}{V_{bed}} \frac{d}{dt} Y_s = -f \tag{15a}$$

$$\varepsilon \rho_g \frac{d}{dt} Y_g + \frac{G_g}{L} \left(Y_g - Y_{g0} \right) = f \tag{15b}$$

where W_{ds} is the dry solid mass.

4.2 – global energy balance

$$\rho_M C_M \frac{dT_M}{dt} + C_{pg} G_g \frac{T_M - T_{g0}}{L} = -f \lambda - E_w \tag{15c}$$

where

$$E_w = \frac{\alpha_w}{V_{bed}} (T_M - T_\infty) \tag{16a}$$

and

$$T_M(t) = \frac{T_g + T_s}{2} \tag{16b}$$

subject to the following initial conditions

$$Y_s(0) = Y_{so} \tag{17a}$$

$$Y_g(0) = Y_{go} \tag{17b}$$

$$T_M(0) = T_{Mo} \tag{17c}$$

The mass transfer rate per volume unit of porous bed is given by

$$f = k_s a\left(Y_s - Y_s^*\right), \tag{18}$$

where the mass transfer coefficient, k_s, was estimated by Vitor (2003), using the three phases model.

5. PARAMETER ESTIMATION

The heat and mass transfer coefficients estimation between interstitial gas and solid phases (Eqs. (15) and (16)), the heat transfer coefficient through bed wall, α_w, and the parameters β_Y and β_T, that quantify the dispersion of the gas in the interstitial phase were estimated by Vitor (2003) and are listed in Tab. 2.

Table 2. Best values of adjustable model parameters.

Parameter	Estimation	Standard deviation.
β_T	1,001	-------
x_1	$1{,}78.10^{-2}$	$2{,}2.10^{-3}$
α_w	$1.32.10^{1}$	$3{,}2.10^{-1}$
β_y	1,49	0,07
x_2	$3{,}76.10^{-2}$	$2{,}8\ .10^{-4}$
x_3	1,177	0,12

$$\mathrm{Nu} = x_1 \mathrm{Re} \tag{19}$$

$$k_s = \frac{D_{ab}}{d_p}\left(x_2 \cdot \mathrm{Re}^{x3}\right) \tag{20}$$

All the drying experiments were conducted in an experimental unit described in Vitor (2003), considering the operational conditions presented in Tab. 3.

Table 3. Operational conditions of experiments.

Exp	*Gg*	*Gg/G$_{gmf}$*	*Tg$_0$*	*Y$_{s0}$*	*L$_f$*
1	0,27	1,17 – 1,64	59	0,231	0,110
2	0,27	1,21 – 1,66	60	0,210	0,108
3	0,29	1,30 – 1,85	75	0,213	0,111
4	0,29	1,31 – 1,76	51	0,207	0,116
5	0, 24	1,11 – 1,44	49	0,192	0,102
6	0,24	1,19 – 1,49	75	0,151	0,098
7	0,27	1,20 – 1,65	61	0,210	0,108
8	0,30	1,31 – 1,82	45	0,224	0,120

Tapioca is a flour derived from manioc. This solid material presents good fluidization, with not very large bubbles, and does not present any solid segregation.

The fluid dynamics properties of the tapioca and of the fluidized bed are listed in Tab. 4

Table 4. Properties of the particles and experimental techniques employed.

Variable	**Method Utilized**
Particle mean diameter $d_p = (88{,}8Y_s + 462{,}8)\ \mu m$	Sieving
Particle Density $\rho_{ss} = 1{,}42 \cdot 10^3\ kg/m^3$	Pycnometry with alcohol (95%) $\rho_s = \frac{\rho_{ss}(1+Y_s)}{1+0{,}70 \cdot Y_s}$
Bed porosity at minimum fluidization $0{,}04 < Y_s < 0{,}22$ e $0{,}42 < \varepsilon_{mf} < 0{,}46$	Volumetry $\varepsilon_{mf} = 1 - \frac{W}{\rho_S L_{mf} A_L}$
Particle mean sphericity $\phi = 0.7$	Permeametry
Isotherm sorption of the tapioca-water-air system $30^oC < T_g < 50^oC$ e $20\% < UR < 70\%$	$Y_s^* = 0{,}19 \cdot UR + 3{,}10 \cdot 10^{-2}$ Mazza and Massarani (2002)
Specific heat of the tapioca particles $C_{ps} = (1{,}55 + 2{,}64 \cdot Y_s^{[bu]}) \cdot 10^3$	Differential Scanning Calorimetry (DSC)

6. RESULTS AND DISCUSSION

The fluidized bed drying of tapioca was modeled by Vitor (2003) using the three phases model previously described. Lima (2004) studied the fluidized bed drying of polyhydroxybutirate (PHB). This material is a biodegradable thermoplastic agent, and its drying process presents an essentially constant drying kinetic rate. In this case the process was modeled by the two phases model. This simplified model was shown to be adequate in this case since the difference between the average temperature of the gas and the temperature of the solid phase is negligible. Based on this fact, the gas and solid phases heat balances were considered as the same and equivalent to an unique well mixed emulsion phase.

During the tapioca drying process conducted in a fluidized bed it was verified that, after the first minutes of the batch process, the difference between the average gas temperature and the solid temperature is negligible. This fact indicates that the same simplification adopted by Lima (2004) could be considered to describe the experiments indicated in Tab. 3. However, it must be emphasized that the three phase model is based on inherent characteristics of the bed, such as: bubbles size; bubble phase porosity and heat and mass transfer rates between the interstitial and bubble gas. On the other hand, the simplified model has very limited predictive capacity and can only be considered as an interpolation model in the range of the experimental data.

The experimental points in the conditions 6, 7 and 8 of Tab. 3 are confronted with the results of the three and two phases modeling of the tapioca drying in Fig. 2. In all the simulations of the three phases model, 20 axial discretization points were adopted; this number of points easily assures, in all the experimental conditions considered, the numerical convergence of the profiles. It should also be pointed out that the physical parameters, common to the both considered models, were estimated adjusting the three phases model to real experimental data. The estimation procedure and statistical analysis of the results is founded in Vitor (2003).

Fig. 2 (a1), (a2) and (a3) present the time variation of the average solid phase moisture. In Fig. 2 (b1), (b2) and (b3) are plotted the time variations of the solid phase temperature in different experimental conditions. Fig. 2 (c1), (c2) and (c3) represent the variations with the time of the gas temperature at the exit of the bed .In all the figures the experimental data obtained are confronted with their correspondent simulated values based on the numerical solutions of the two and three phases models.

7. CONCLUSION

The results obtained through the numerical resolution of the two models show, Fig. 2, that both models reasonably adjust the experimental data. This demonstrates that the simplifying hypotheses of the two phase model are quite reasonable to describe the fluidized bed drying of the tapioca in the conditions studied. However, these results also show that the available experimental data can not be used to discriminate which of the two models is more adequate to describe the process. This decision can only be taken if local measurements inside the bed, moisture and temperature

profiles of all existing phases, were available. This way, the discrepancy observed between the solutions of both models can be justified by the highest accuracy of the three-phase model.

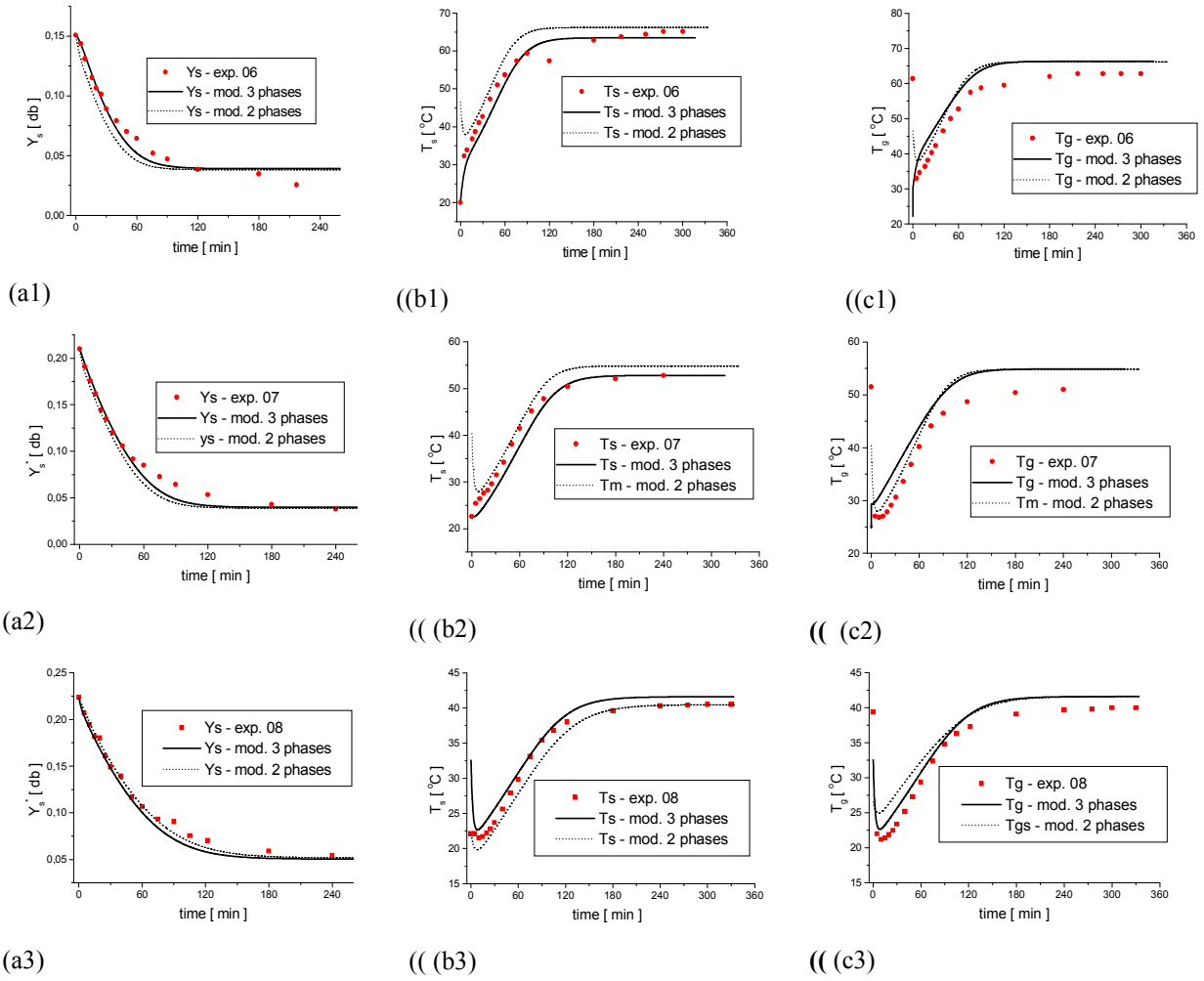

Figure 2. Comparison between simulated and experimental data: (a) drying curve; (b) solid temperature; (c) outlet air temperature (tests 6, 7 and 8; see Tab. 3).

The two models demonstrate better adjustment to the solid phase experimental data in comparison with the adjustment capacity of the gas phases properties. Another aspect that should be pointed out is the offset presented between the measured gas outlet temperature and the same value predicted by both models. Such difference probably occurs due to the inherent measurement difficulties of this temperature. The difference of the gas temperature in the beginning of the drying - in the conditions of the experiments 6 and 7 - are due to the abrupt introduction of the initial conditions of the problem. During the measurements, to avoid the solid collisions, the thermocouple was enveloped inside a 100 mesh screen. The inherent heat capacity of this screen can produce, during dynamic temperature measurements, a time delay that makes the temperatures effectively measured by the iron-constantan thermocouple time delayed from the real one. The inclusion to the mathematical model of a single first order dynamic with an adjusted time constant will certainly reduce this measurement error.

8. REFERENCES

Biscaia Jr, E. C. and Massarani, G.; Pinto, J. C., “Secagem de Grãos: Modelo a Duas Fases”, Proceedings of Conbea in CD Rom (1996).

Calado, V. M. A., “Modelagem e Simulação de Secadores em Leito Fixo e Deslizante”, D.Sc. Thesis, Coppe/Ufrj, Brazil (1993).

Calçada, L. A., "Modelagem e Simulação de Secadores em Leito Fixo", M.Sc. Thesis, Coppe/Ufrj, Brazil (1994).
Calçada, L. A., "Secagem de Materiais Granulares Porosos", D.Sc. Thesis, Coppe/Ufrj, Brazil (1998).
Hilligardt, K. and Werther, J., "Local Bubble Gas Hold-up and Expansion of Gas/Solid Fluidized Beds", Germ. Chem. Engn., 9, pp. 215-221 (1986).
Hoebink, J. H. B. J. and Rietema, K., "Drying Granular Solids in Fluidized Bed I. Description on Basis of Mass and Heat Transfer Coefficients", Chem. Engn. Science, 35, pp. 2135-2140 (1980-a).
Hoebink, J. H. B. J. and Rietema,K., "Drying Granular Solids in Fluidized Bed II. The Influence of Diffusion Limitation on the Gas-Solid Contacting around bubbles", Chem. Engn. Science, 35, pp. 2257-2265 (1980-b).
Kerkhof, P. J. A. M., "Relations Between Local and effective Air-Side Mass and Heat Transfer Coefficients in Fluidized-Bed Drying", Drying Technology, 12, pp. 1191-1210 (1994).
Kunii, D. and Levenspiel, O., "Fluidization Engineering", Butterworth-Heinemann, USA (1991).
Lima, O. A., "Estudo da Secagem do Polihidroxibutirato (PHB) em Leito Fluidizado", M.Sc. Thesis, Coppe/Ufrj, Brazil (2004).
Massarani, G., "Fluidodinâmica em Sistemas Particulados", Ed. UFRJ, Brazil (1997)
Mazza, M. and Massarani, G., "Análise de um Sistema para Levantamento de Isotermas II", COBEQ (2002).
Mancini, M. C., "Transferência de Massa em Secadores de Grãos", D.Sc. Thesis, Coppe/Ufrj, Brazil, (1996).
Pakowski, Z., Barczak Z., Strumilo C. and Stenstrom S., "Evaluation of Equations Approximating and Transport Properties of Water, Steam and Air for Using CAD of drying Process", Drying Technology, 9, No.3, pp. 753-773. (1991),
Palàncz, B., "A Mathematical Model for Continuous Fluidized Bed Drying", Chem. Engn. Science, 38, No.7, pp. 1045-1059 (1982).
Petzold, L. R., "DASSL: A Differential-Algebraic System Solver, Computer and Mathematical Research Division", Lawrence Livermore National Laboratory, Livermore, CA, USA (1989).
Rizzi, A.C., Costa jr., E.F., Freire, J.T., and Passos, M.L., " Modeling the Drying of Grass Seeds (Brachiaria Brizantha) in Fluidized Bed", Drying Technology, 25, pp. 123-134 (2007).
Truesdell, C., Sulle Basi della Termomeccanica, cited by Silva Telles A. and Massarani G., 1991, "Sistemas Particulados a Duas Fases Multicomponentes", Annals of the XIX Encounter on Outflow in Porous Mediums, vol. I, pp. 91-101 (1957).
Valença, G. C. and Massarani, G., "Grain drying in countercurrent and concurrent gas flow-modeling", simulation and experimental results, *Drying technology,* 18, pp. 447-455 (2000).
Vitor, J. F. A. V., Modelagem da Secagem de Biomassa em Leito Fluidizado, D. Sc. Thesis, Coppe/Ufrj, Brazil, (2003).
Wang, Z. H. and Chen, G., "Heat and Mass Transfer in Batch Fluidized-Bed Drying of Porous Particles", Chem.Engn.Science, 55, pp. 1857-1869 (2000).
Wildhagen, G. R. S., Calçada, L. A. and Massarani, G., "Drying of Porous Particles in Fluidized Beds: Modeling and Experiments", Journal of Porous Media, 5, No.2, pp. 123-133 (2002).
Zahed, A. H., Zhu, J. X. and Grace, J. R., "Modeling and Simulation of Batch and Continuous Fluidized-Bed Dryers", Drying Technology, 13, pp. 1-28 (1995).

9. RESPONSIBILITY NOTICE

The authors are the only responsible for the printed material included in this paper.